Bio-Polymer Based Tragacanth Gum (TG) Loaded Fe₃O₄ Nanocomposite for the Sequestration of Tenacious Congo Red Dye from Waste Water

Arush Sharma[1], Deepak Pathania[2,3,*] and Ajay Kumar[4]

[1]*Department of Chemistry, Baddi University of Emerging Sciences and Technology, Solan, Himachal Pradesh, 173205, India*

[2]*Department of Environmental Science, Central University of Jammu, Bagla (Rahya-Suchani), Samba, Jammu & Kashmir, 181143, India*

[3]*Department of Chemistry, Sardar Vallabhbhai Patel Cluster University, Mandi, Himachal Pradesh, 175001, India*

[4]*Shoolini Institute of Life Sciences and Business Management (SILB), Solan, India*

Abstract: Water polluted by hazardousdyes such as congo red (CR) face challenges to the regulation of water supplies. In the laboratory scale experiment, we report the novel approach for the synthesis of Fe_3O_4/TG nanocomposite. The Fe_3O_4/TG nanocomposite was synthesized by co-precipitation method. The surface properties and chemical compositions have been investigated using Fourier transform infrared spectroscopy (FTIR), X- ray diffractometer (XRD), scanning electron microscope (SEM), transmission electron microscope (TEM) instrumentation. The XRD study indicates that nanocomposite were formed in the nano-scale (11.5 nm) and this is in accordance with TEM results. The maximum removal of CR dye was recorded at 2.0 pH. Approximately, 89.51 % deterioration of congo red (CR) dye has been achieved within 250 min of solar exposure. The prepared Fe_3O_4/TG nanocomposite is found to efficient photocatalyst for the removal of noxious dye from waste water.

Keywords: Bio-polymer, Tragacanth gum (TG), Characterization, Fe_2O_3, Photo-catalysis, Dye.

INTRODUCTION

Contamination of surface water and groundwater with aromatic compounds is one of the most extreme environmental issues. Water scarcity has been an exigent concern in most of regions of world due to dearth of water supplies, population explosion, toxic waste, irrational consumption and climate changes. Wastewater from textile, paper, plastics, chemical, petroleum products markets, etc. produce a brew of poisonous and non-biodegradable chemical contaminants [1-5]. The need for water purification to ensure quality drinking and availability, has thus increased.

Synthetic dyes are widely used in numerous branches of the garment industry, paper processing, colour imaging, pharmaceutical, leather, cosmetics, rubber, and other industries. The discharges of industrial wastewater containing dyes pose severe environmental issues because of its high toxicity and potential accumulation in the environment [6-10]. There are more than 100,000 different synthetic dyes available in the market with total production of 700,000 tons annually worldwide. About, 1-20% of the total world production of dyes is lost during the dyeing process and released in the textile effluents. The release of colored wasteto the environment has proven to be considerable source of non-aesthetic pollution. Most of the synthetic dyes have mutagenic, carcinogenic and recalcitrant effect on human body [11-13]. Therefore, removal of color from these effluents has poses major problem of our ecological system.

Among various dyes, congo red (CR) is a secondary diazo dye. Congo red contains an azo (-N=N-) chromophore and acidic oxochrome. Congo red is the sodium salt of a derivative of benzidine and naphthionic acid [14-15]. It is water soluble, yielding a red colloidal solution. It has a strong, though apparently non-covalent affinity to cellulose fibers. It has tendency to change colour when touched by sweaty fingers because of its toxicity. It is also used to colour the textiles. A number of attempts have been made for the treatment of wastewater using various physical and chemical methods. The traditional physical techniques for de-colorization such as adsorption, ultra-filtration, reverse osmosis, coagulation by chemical agents and ion exchange on synthetic adsorbent resins etc. are efficiently used.

Among all the possible methods of de-colorization for the textile wastewater, photo catalytic treatment seems to be promising and effective because, it involves the degradation of pollutant from wastewater. Due to the large degree of aromatics present in the dye molecules and the stability of modern dyes, the conventional biological methods are ineffective [16]. The heterogeneous photocatalysis has long been known to be an environmental-friendly technology to combat more and more emerging environmental problem [17-19].

Nanocomposite technology is a newly developed field, in which nano-particle are added to a polymer to reinforce and to provide the novel characteristics. Nanocomposite technology is applicable to a wide range of polymers. Nanocomposites differ from the conventional composite materials due to exceptionally high surface to volume ratio. Iron nanoparticles (Fe_2O_3) are highly useful for amputation of organic pollutants from waste water because they can donate electrons to more electronegative atoms, such as chlorine atoms, present in many of molecules of organic pollutants [20-23]. Donating electrons cause the molecules to break up into harmless molecules. Because nanoparticles can remain suspended in groundwater for a long time and transported throughout the system. They are used to treat large areas of ground water.

Tragacanth is a natural gum obtained from the dried sap of a number of species of middle eastern legumes species. The gum is occasionally called, gumshiraz, gum elect or gum dragon. Iran is the world biggest manufacturer of this gum. Tragacanth gum (TG) is a viscous, odorless and tasteless. It is the mixture of polysaccharides, soluble in water, obtained from sap tired from the root of the plant and dried up. Tragacanth has been used as a demulcent in cough and cold to manage diarrhea. It has been used as a topical treatment of burns. It is used in pharmaceuticals and foods as an emulsifier, stabilizer and texturant additive that do not generally change the flavor. It is the binder used in the making of artists' pastels.

With the discussion on aforementioned point, our prime aim is to synthesize the Fe_2O_3/TG nanocomposites using simple co-precipitation method. The prepared nanocomposite has been explored for the removal of tenacious cong red (CR) dye from waste water. The Fe_2O_3/TGnanocomposite has been characterized using various instrumental techniques such as Fourier transform infrared spectroscopy (FTIR), X- ray diffractrometer (XRD), scanning electron microscopy (SEM), transmission electron microscopy (TEM).

2. MATERIALS AND METHODS

2.1. Materials

Ferric chloride hexahydrate ($FeCl_3·6H_2O$), ferric chloride tertahydrate ($FeCl_2·4H_2O$), ammonium hydroxide (NH_4OH) and tragacanth gum (TG) were purchased from Central Drug House (CDH) Private Lt. India. All chemicals were used without further purification. Glass wares were washed with water and rinsed with acetone and then dried.

2.2. Synthesis of Fe₃O₄ Nanoparticle

Fe_3O_4 nanoparticles were synthesized by co-precipitation method. In this method $FeCl_3·6H_2O$ (0.1M) and $FeCl_2·4H_2O$ (0.1M) at the molar ratio of 2:1 were mixed. After stirring for 10 minutes, NH_4OH (1 M) was added to the solution with continuous shaking. Black precipitate appeared. Then solution was stirred for 2h at 50°C. The Fe_3O_4 precipitates were separated centrifugally at 2500 rpm for 5 minutes and then dried at 50°C.

2.3. Synthesis of Fe₃O₄ /TG Nanocomposite

Fe_3O_4/TG nanocomposite was synthesized by co-precipitation method. In this method, $FeCl_3·6H_2O$ (0.1M) and $FeCl_2·4H_2O$ (0.1M) at the molar ratio of 2:1 were mixed. After stirring for 10 minute, NH_4OH (1 M) was added to the solution with continuous shaking. Black precipitate has been formed. After that, the solution of tragacanth gum (1g) was prepared in 40 mL of distilled water and added drop wise into above prepared solution with stirring. The resultant mixture was stirred for 2h at 50°C. The precipitates were separated centrifugally at 2500 rpm for 5 minutes and then dried at 50°C.

2.4. Photocatalytic Degradation of CRdye

Congo red ($C_{32}H_{22}N_6Na_2O_6S_2$, Molecular weight: 696.67) was used as a model dye to investigate the photocatalytic activity of Fe_3O_4/TG nanocomposite. In the 100 mg, of nanocomposite was added into 60 mL solution of congo red in 250 mL beaker. Initially, degradation of the reaction mixture was noticed in dark for 60 minute before exposed to solar light (Scheme **1**). Then degradation of reaction mixture was checked in the presence sun light for 80 min. The changes in the concentration of both the solutions were recorded at
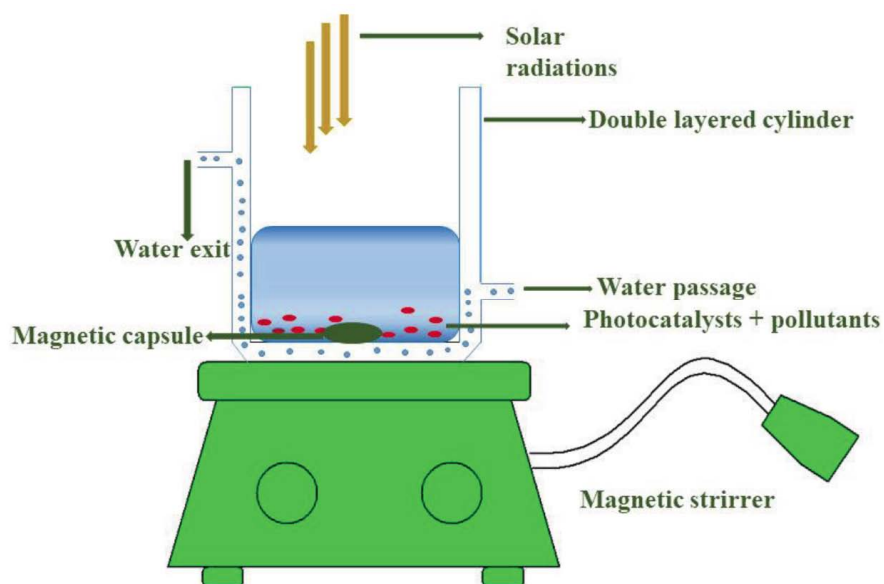
Scheme1: Photocatalytic Experimental set-up.

497 nm using UV-vis spectrophotometer [24]. The % degradation was checked using following equation:

% degradation $= \dfrac{c_0 - c_t}{c_0} \times 100$

Where c_0 is the initial absorbance and c_t is the absorbance at time

The rate of photodegradation reaction was studied using pseudo first order kinetics by plotting graph between the values of log $\dfrac{A_0}{A}$ with time and the rate constant was calculated as:

K=2.303× log $\dfrac{A_0}{A}$

Where log $\dfrac{A_0}{A}$ is the slope

2.5. Characterization

Instrumental techniques such as Fourier transform infrared spectroscopy (FTIR), X- ray diffractrometer (XRD), scanning electron microscopy (SEM), transmission electron microscopy (TEM) has been used. Fourier transform infrared spectroscopy (FTIR) is a powerful analytic technique provides information about the structure and bonding of the molecule. FTIR analysis was carried in the wave number ranged from 4000cm^{-1} to 400cm^{-1} using infrared spectrophotometer (Perkin Elmer Spectrum, 400). FTIR spectrum was recorded using KBr disk method. In this 10 mg of

nanocomposite was mixed with 100 mg of KBrand then appropriate phenomena exerted to from transparent disc. Scanning electron microscopy (SEM) studyhas been performed using NOVA NANOSEM 450 scanning electron microscope with an image accelerating voltage of 20 KV to determine the morphology of particles. In this technique, imageof the sample is determinedusing high- energy electron beam. TEM produces a high resolution, black and white image from the interaction that takes place between prepared sample and energetic electrons in the vacuum chamber. TEM provide the topographical, morphological, compositional and crystalline information of the nanocomposite. The crystallinity and size of nanocompositehas been determined using X-ray diffractometer using CuKα radiation.

3. RESULTS AND DISCUSSIONS

3.1. FTIR Study

FTIR spectrum of tragacanth gum is shown in the Figure **1a**. The stretching vibration of -OH group of tragacanth gum appears at 3334 cm^{-1}. The asymmetric stretching vibration of the methylene group was assigned at 2910 cm^{-1}. The characteristic peaks at 1603 cm^{-1} and 1421 cm^{-1} were due to C=O stretching vibrations of carboxylic acid. The C-O stretching vibrations of alcoholic groups were appeared at 1255 cm^{-1} and 1043 cm^{-1}. FTIR spectrum of Fe_3O_4/TG nanocomposite has been shown in Figure **1b**. The stretching vibrations of -OH were located between 3500 cm^{-1} and 3000 cm^{-1}. The characteristic peaks at
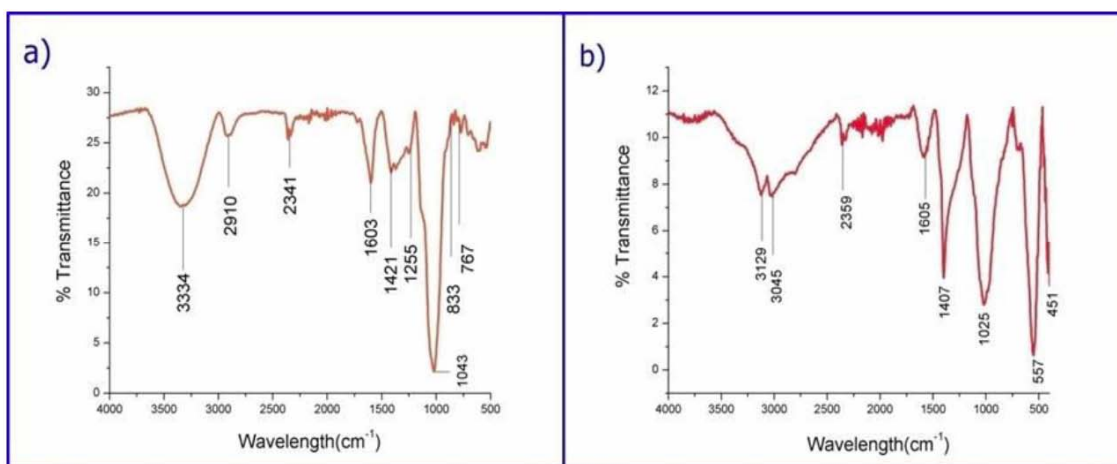
Figure 1: (a) FTIR spectrum of tragacanth gum & **(b)** FTIR spectrum of Fe₃O₄/TG.

1605 cm^{-1} and 1407 cm^{-1} were due to C=O stretching vibrations of carboxylic acid. The C-O stretching vibrations of alcoholic group appeared at 1025 cm^{-1}. The stretching frequenciesof Fe₃O₄signal in the nanocomposite has been observedbetween 600-540 cm^{-1} [25-27].

3.2. Scanning Electron Microscope (SEM) Study

SEM images of Fe₃O₄ nanoparticle and Fe₃O₄/TGnanocomposite are shown in the Figure **2a-d**.

This was clear from the SEM images that synthesized sample possess cuboidal, and cylindrical structure.

3.3. Transmission Electron Microscope (TEM) Analysis

TEM images of Fe₃O₄ nanoparticle and Fe₃O₄/TGnanocomposite is given in the Figure **3a-d**. The particles are spherical in shape and there is uniform distribution of nanoparticles.However, agglomerate clusters have been observed. There were
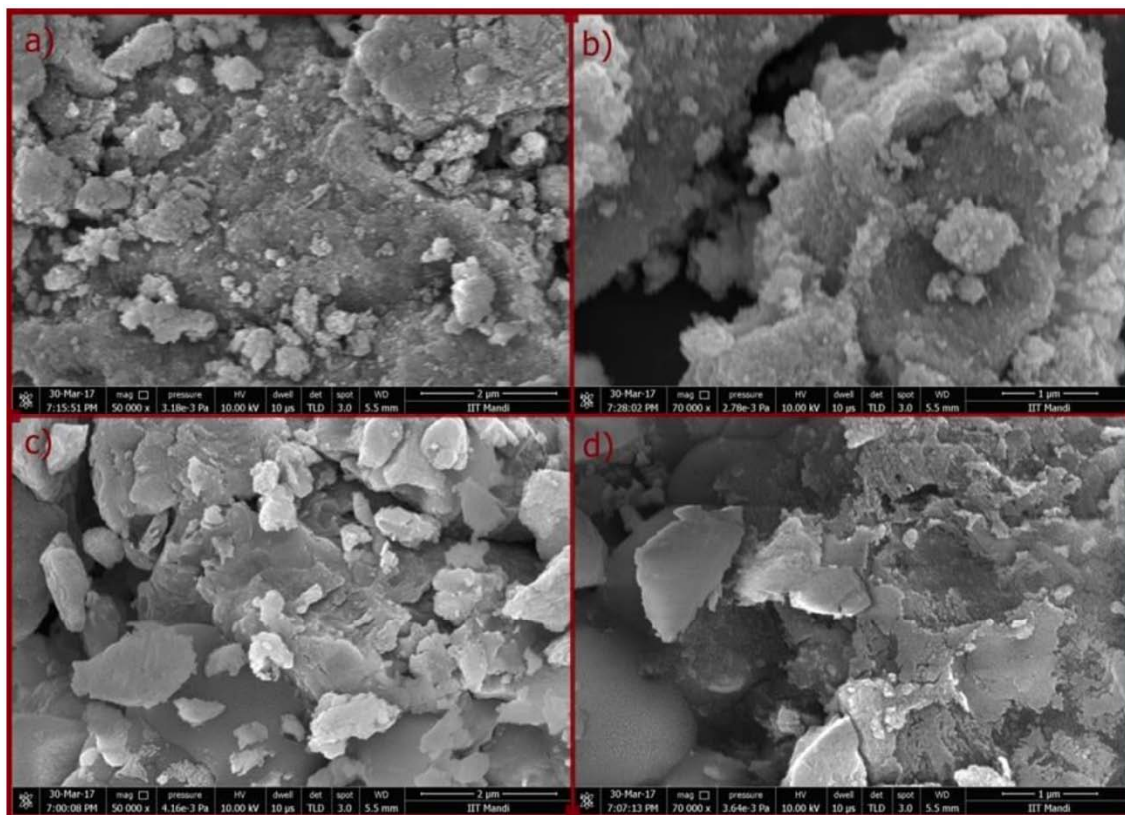
Figure 2: (a-b) SEM images of Fe₃O₄ nanoparticle &**(c-d)** Fe₃O₄/TGnanocomposite.
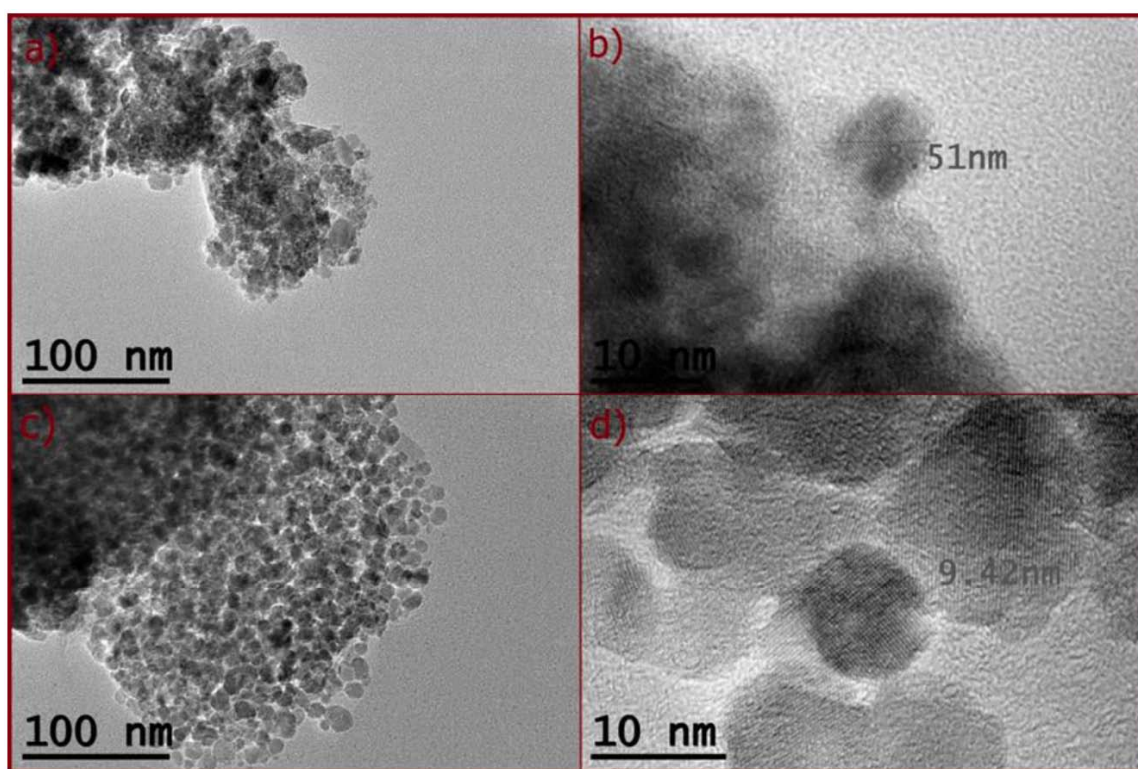
Figure 3: (**a-b**) TEM images of Fe_3O_4 nanoparticle & (**c-d**) Fe_3O_4/TG nanocomposite.

bimodal particle size distribution of Fe_3O_4/TGnanocomposite with two average size. The black core represents the Fe_3O_4 particles. The average particle size of Fe_3O_4/TGnanocomposite has found to be 10 nm.

3.4. X-Ray Diffraction Studies (XRD)

The XRD pattern of Fe_3O_4/TG nanocomposite is presented in the Figure **4**. The d-spacing is calculated using Bragg's law [28-29].
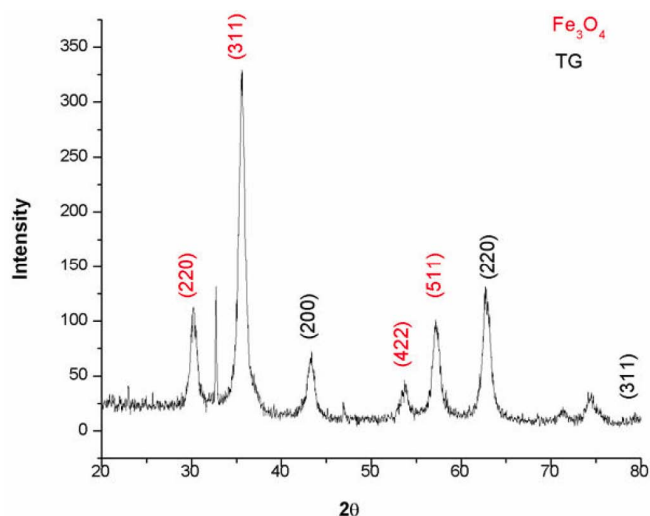
Figure 4: XRD pattern of Fe_3O_4/TG nanocomposite.

$n\lambda = 2d\sin\theta$

Where λ = wavelength of X-ray, d = inter planar spacing, θ = diffraction angle n = 0, 1, 2, 3, etc.

The average particle size of synthesized materials was obtained from XRD measurement value of FWHM using Debye-Scherrer's formula [30-32];

$$D = \frac{K\lambda}{\beta\cos\theta}$$

Where K is constant (0.9), λ is wavelength (λ=1.54Å), β is full width at half maximum intensity (FWHM) and θ is the half diffraction angle.The lattice constants for spinel cubic structure were calculated by using the formula;

$$d_{hkl} = \frac{a}{\sqrt{h^2 + k^2 + l^2}}$$

The characteristics peaks for Fe_3O_4 at 2θ angle at $29.98°$, $35.73°$, $53.68°$, and $57.14°$ correspond to (220), (311), (422), (511) diffraction planes with standard JCPDS file no. 65-3107. For TG the 2θ angle at $43.34°$, $63.15°$, $79.33°$ corresponds to (200), (220) and (311) diffraction plane with standard JCPDS file no. 04-0783. The Fe_3O_4 follows the cubic crystal lattice.The lattice constants are calculated (Tables **1** and **2**). The particle

Table 1:   d Spacing of Fe₃O₄/TG Nanocomposite

Sr. No.	2θ (in degrees)	Diffraction planes for Fe₃O₄	d-spacing (Å)	Diffraction planes for TG	d-spacing (Å)
1	29.98˚	(220)	1.17		
2	35.73˚	(311)	2.52		
3	43.34˚			(200)	2.10
4	53.68˚	(422)	1.70		
5	57.14˚	(511)	1.61		
6	63.15˚			(220)	1.47
7	79.33˚			(311)	1.21

Table 2:   Lattice Parameters of Fe₃O₄ Nanoparticle

| Lattice Parmeter	Lattice conatants	Structure	JCPDS no.
Fe₃O₄	a = 0.480nm	Cubic	65-3107

size calculated from XRD study was found to be 11.5 nm.

3.5. Photo Catalysis

UV-Vislight absorption spectra were recorded at 497nm. The Fe₃O₄/TGnanocomposite should substantially improve its response in the visible region. Prior to the experiment of photocatalytic, there are two experiments conducted. The first part of the experiment was conducted in dark. Under dark condition, approximate 20.20 % of dye has been removed within 60 min. After this,reaction mixture was exposed to solar light. The maximum removal of CR dye has found to be 89.51 %within 250 min (Figure **5**). The rate of photo degradation reaction was studied using pseudo first order kinetics (Figure **6**). The linear fit graph has higher value of regression coefficient (R^2=0.95). The value of rate constant K = 0.0459 min^{-1} was calculated from the slope of the plot.
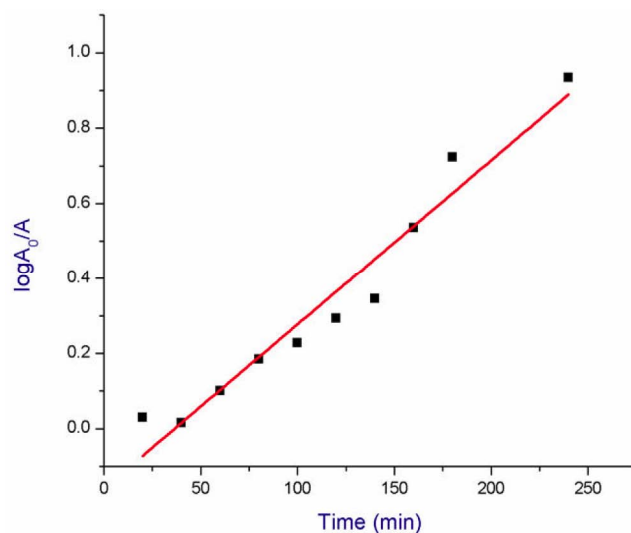
Figure 6: Pseudo first order kinetics for CR dye.

The effect of pH on the degradation of CR dye has been also investigated in the range of 2.0 to 12.0 pH. The maximum removal of CR dye has been observed at 2.0 pH.This may be due to the electrostatic interaction between nanocomposite and negative charged dye molecules. While at higher pH repulsive interaction takes place, which corresponds to lesser removal of dye molecules. The detailed mechanism of

Figure 5: Degradation (%) of congo red dye in dark and sunlight.

CR degradation using nanocomposite has been presented in the Figure **7**.
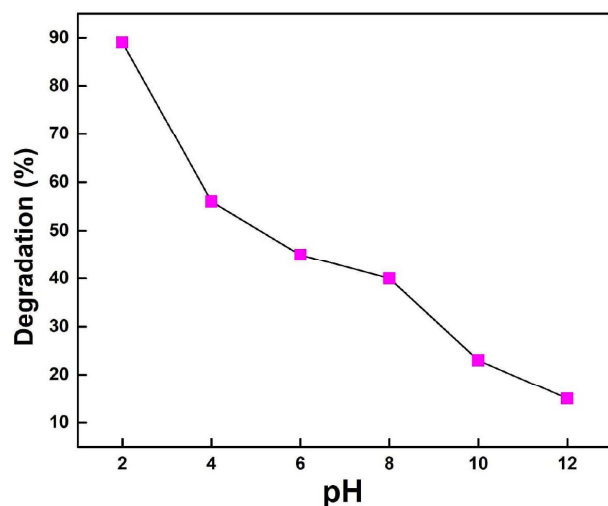
Figure 7: Effect of pH on degradation of CR dye byFe$_3$O$_4$/TG nanocomposite.

4. CONCLUSIONS

In this study, a simple co-precipitation method was employed to synthesize the magnetic Fe$_3$O$_4$

nanocomposites at 50°C.We have synthesized the Fe$_3$O$_4$/TG nanocomposite. The nanocomposite was characterized by UV-spectrometer, X-ray diffractrometer (XRD), Fourier transform electron spectroscopy (FTIR), Scanning electron microscopy (SEM) and transmission electron microscopy (TEM). The characterization confirmed the formation of desired Fe$_3$O$_4$/TG nanocomposite. The nanocomposites proved to be better agent for the removal of organic pollutants. The photo catalytic activity of synthesized nanomaterials was evaluated by photo degradation of congo red dye. Approximate, 90 % of CR dye has been photodegraded using Fe$_3$O$_4$/TG nanocomposite, Hence, study offered a novel approach to design efficient and stable photocatalyst for the elimination of persistent organicpollutant from waste water.

CONFLICT OF INTEREST

Authors declare no conflict of interest among them.

ACKNOWLEDGEMENT
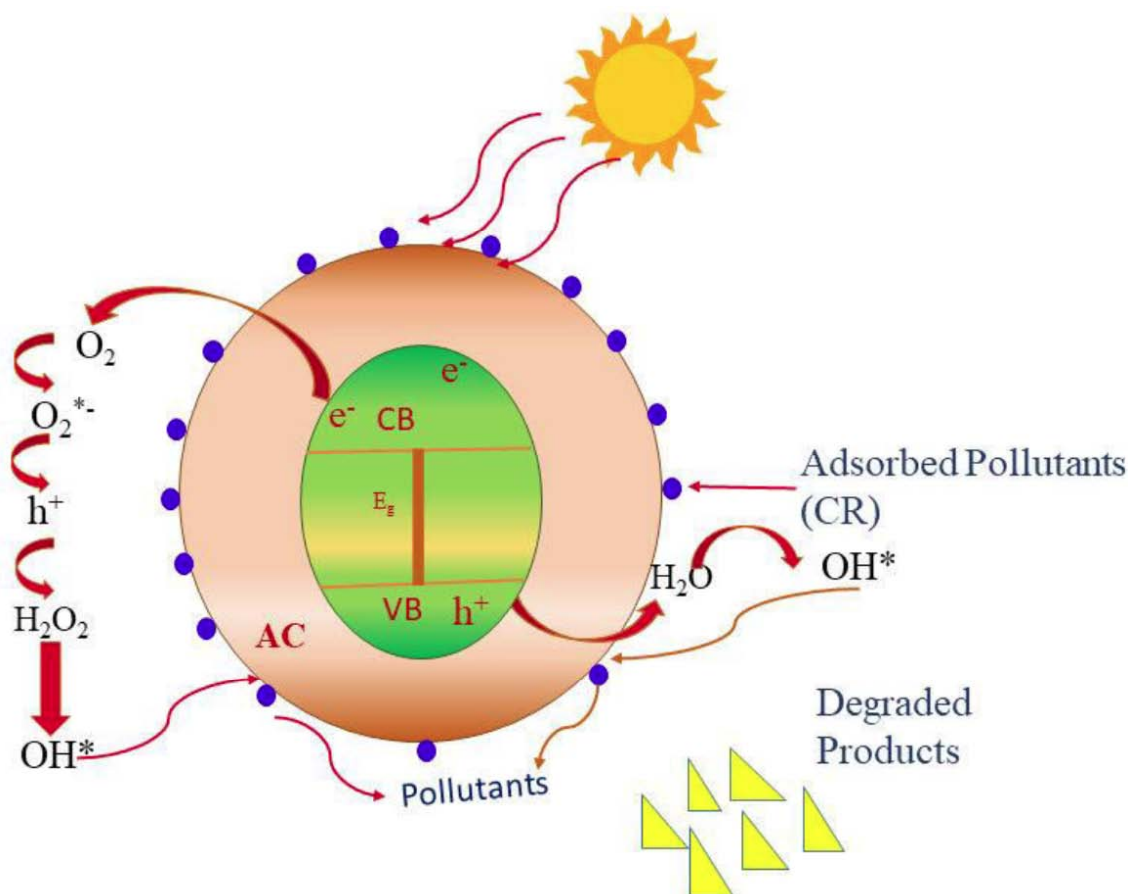
Figure 8: Schematic representation of photodegradation of CR dye.

REFERENCES

[1]   Bhatnagar A, Anastopoulos I. Adsorptive removal of bisphenol A (BPA) from aqueous solution: a review. Chemosphere 2017; 168: 885-902.
https://doi.org/10.1016/j.chemosphere.2016.10.121

[2]   Sharma A, Siddiqi ZM, Pathania D. Adsorption of polyaromatic pollutants from water system using carbon/ZnFe2O4 nanocomposite: equilibrium, kinetic and thermodynamic mechanism. Journal of Molecular Liquids 2017; 240: 361-371.
https://doi.org/10.1016/j.molliq.2017.05.083

[3]   Aryee AA, Mpatani FM, Kani AN, Dovi E, Han R, Li Z, Qu L. Iminodiacetic acid functionalized magnetic peanut husk for the removal of methylene blue from solution: characterization and equilibrium studies. Environmental Science and Pollution Research 2020; 27(32): 40316-40330.
https://doi.org/10.1007/s11356-020-10087-6

[4]   Aryee AA, Mpatani FM, Zhang X, Kani AN, Dovi E, Han R, Li Z, Qu L. Iron (III) and iminodiacetic acid functionalized magnetic peanut husk for the removal of phosphate from solution: characterization, kinetic and equilibrium studies. Journal of Cleaner Production 2020; 268: 122191.
https://doi.org/10.1016/j.jclepro.2020.122191

[5]   Aryee AA, Mpatani FM, Du Y, Kani AN, Dovi E, Han R, Li Z, Qu L. Fe3O4 and iminodiacetic acid modified peanut husk as a novel adsorbent for the uptake of Cu (II) and Pb (II) in aqueous solution: Characterization, equilibrium and kinetic study. Environmental Pollution 2021; 268: 115729.
https://doi.org/10.1016/j.envpol.2020.115729

[6]   Belfroid A, van Velzen M, van der Horst B, Vethaak D. Occurrence of bisphenol A in surface water and uptake in fish: evaluation of field measurements. Chemosphere 2002; 49(1): 97-103.
https://doi.org/10.1016/S0045-6535(02)00157-1

[7]   Bhattacharyya KG, Sharma A. Azadirachtaindica leaf powder as an effective biosorbent for dyes: a case study with aqueous Congo Red solutions. Journal of Environmental Management 2004; 71(3): 217-229.
https://doi.org/10.1016/j.jenvman.2004.03.002

[8]   Afkhami A, Moosavi R. Adsorptive removal of Congo red, a carcinogenic textile dye, from aqueous solutions by maghemite nanoparticles. Journal of Hazardous Materials 2010; 174(1-3): 398-403.
https://doi.org/10.1016/j.jhazmat.2009.09.066

[9]   Pathania D, Sharma A, Siddiqi ZM. Removal of congo red dye from aqueous system using Phoenix dactylifera seeds. Journal of Molecular Liquids 2016; 219: 359-367.
https://doi.org/10.1016/j.molliq.2016.03.020

[10]   Sharma A, Thakur KK, Mehta P, Pathania D. Efficient adsorption of chlorpheniramine and hexavalent chromium (Cr (VI)) from water system using agronomic waste material. Sustainable Chemistry and Pharmacy 2018; 9: 1-11.
https://doi.org/10.1016/j.scp.2018.04.002

[11]   Sharma A, Siddiqui ZM, Dhar S, Mehta P, Pathania D. Adsorptive removal of congo red dye (CR) from aqueous solution by Cornulacamonacantha stem and biomass-based activated carbon: isotherm, kinetics and thermodynamics. Separation Science and Technology 2019; 54(6): 916-929.
https://doi.org/10.1080/01496395.2018.1524908

[12]   Sharma A, Sharma G, Kumar A, Siddiqi ZM. Exclusion of organic dye using neoteric activated carbon prepared from cornulacamonacantha stem: equilibrium and thermodynamics studies. In Materials Science Forum. Trans Tech Publications Ltd. 2016; Vol. 875: pp. 1-15.
https://doi.org/10.4028/www.scientific.net/MSF.875.1

[13]   Kumar A, Pathania D, Gupta N, Raj P, Sharma A. Photo-degradation of noxious pollutants from water system using Cornulacamonacantha stem supported ZnFe2O4 magnetic bio-nanocomposite. Sustainable Chemistry and Pharmacy 2020; 18: 100290.
https://doi.org/10.1016/j.scp.2020.100290

[14]   Bhatti HN, Mahmood Z, Kausar A, Yakout SM, Shair OH, Iqbal M. Biocomposites of polypyrrole, polyaniline and sodium alginate with cellulosic biomass: Adsorption-desorption, kinetics and thermodynamic studies for the removal of 2, 4-dichlorophenol. International Journal of Biological Macromolecules 2020; 153: 146-157.
https://doi.org/10.1016/j.ijbiomac.2020.02.306

[15]   Bhaumik M, McCrindle R, Maity A. Efficient removal of Congo red from aqueous solutions by adsorption onto interconnected polypyrrole–polyaniline nanofibres. Chemical Engineering Journal 2013; 228: 506-515.
https://doi.org/10.1016/j.cej.2013.05.026

[16]   Pathania D, Dhar S, Sharma A, Srivastava AK. Decolourization of noxious safranin-T from waste water using Mangiferaindica as precursor. Environmental Sustainability 2020; 1-10.
https://doi.org/10.1007/s42398-020-00130-0

[17]   Sharma A, Sood S, Pathania D. Remedial Role of Nanocomposite as Photocatalysts, Adsorbents, and Disinfectants in Aqueous System and Their Biomedical Applications. In Metabolic Engineering for Bioactive Compounds. Springer, Singapore 2017; pp. 371-401.
https://doi.org/10.1007/978-981-10-5511-9_18

[18]   Ho W, Zhang Z, Lin W, Huang S, Zhang X, Wang X, Huang Y. Copolymerization with 2, 4, 6-triaminopyrimidine for the rolling-up the layer structure, tunable electronic properties, and photocatalysis of g-C3N4. ACS Applied Materials & Interfaces 2015; 7(9): 5497-5505.
https://doi.org/10.1021/am509213x

[19]   Chen B, Meng Y, Sha J, Zhong C, Hu W, Zhao N. Preparation of MoS 2/TiO 2 based nanocomposites for photocatalysis and rechargeable batteries: progress, challenges, and perspective. Nanoscale 2018; 10(1): 34-68.
https://doi.org/10.1039/C7NR07366F

[20]   Yin L, Shen Z, Niu J, Chen J, Duan Y. Degradation of penta-chlorophenol and 2, 4-dichlorophenol by sequential visible-light driven photocatalysis and laccase catalysis. Environmental Science & Technology 2010; 44(23): 9117-9122.
https://doi.org/10.1021/es1025432

[21]   Liu J, Wang H, Antonietti M. Graphitic carbon nitride "reloaded": emerging applications beyond (photo) catalysis. Chemical Society Reviews 2016; 45(8): 2308-2326.
https://doi.org/10.1039/C5CS00767D

[22]   Ren L, Li Y, Hou J, Bai J, Mao M, Zeng M, Zhao X, Li N. The pivotal effect of the interaction between reactant and anatase TiO2 nanosheets with exposed {0 0 1} facets on photocatalysis for the photocatalytic purification of VOCs. Applied Catalysis B: Environmental 2016; 181: 625-634.
https://doi.org/10.1016/j.apcatb.2015.08.034

[23]   Kuang Y, Wang K, Shi X, Huang X, Meggers E, Wu J. Asymmetric Synthesis of 1, 4-Dicarbonyl Compounds from Aldehydes by Hydrogen Atom Transfer Photocatalysis and Chiral Lewis Acid Catalysis. Angewandte Chemie International Edition 2019; 58(47): 16859-16863.
https://doi.org/10.1002/anie.201910414

[24]   Pathania D, Sharma A, Srivastava AK. Modelling studies for remediation of Cr (VI) from wastewater by activated Mangiferaindica bark. Current Research in Green and Sustainable Chemistry 2020; 3: 100034.
https://doi.org/10.1016/j.crgsc.2020.100034

[25]   Do BPH, Nguyen BD, Nguyen HD, Nguyen PT. Synthesis of magnetic composite nanoparticles enveloped in copolymers specified for scale inhibition application. Advances in Natural Sciences: Nanoscience and Nanotechnology 2013; 4(4): 045016.
https://doi.org/10.1088/2043-6262/4/4/045016

[26]   Gupta H, Kumar R, Park HS, Jeon BH. Photocatalytic efficiency of iron oxide nanoparticles for the degradation of priority pollutant anthracene. Geosystem Engineering 2017; 20(1): 21-27.
https://doi.org/10.1080/12269328.2016.1218302

[27]   Bhosale SS, Rohiwal SS, Chaudhary LS, Pawar KD, Patil PS, Tiwari AP. Photocatalytic decolorization of methyl violet dye using Rhamnolipidbiosurfactant modified iron oxide nanoparticles for wastewater treatment. Journal of Materials Science: Materials in Electronics 2019; 30(5): 4590-4598.
https://doi.org/10.1007/s10854-019-00751-0

[28]   Shamaila S, Bano T, Sajjad AKL. Efficient visible light magnetic modified iron oxide photocatalysts. Ceramics International 2017; 43(17): 14672-14677.
https://doi.org/10.1016/j.ceramint.2017.07.193

[29]   Bishnoi S, Kumar A, Selvaraj R. Facile synthesis of magnetic iron oxide nanoparticles using inedible Cynometraramiflora fruit extract waste and their photocatalytic degradation of methylene blue dye. Materials Research Bulletin 2018; 97: 121-127.
https://doi.org/10.1016/j.materresbull.2017.08.040

[30]   Vasantharaj S, Sathiyavimal S, Senthilkumar P, LewisOscar F, Pugazhendhi A. Biosynthesis of iron oxide nanoparticles using leaf extract of Ruelliatuberosa: antimicrobial properties and their applications in photocatalytic degradation. Journal of Photochemistry and Photobiology B: Biology 2019; 192: 74-82.
https://doi.org/10.1016/j.jphotobiol.2018.12.025

[31]   Kannan K, Radhika D, Nikolova MP, Sadasivuni KK, Mahdizadeh H, Verma U. Structural studies of bio-mediated NiO nanoparticles for photocatalytic and antibacterial activities. Inorganic Chemistry Communications 2020; 113: 107755.
https://doi.org/10.1016/j.inoche.2019.107755

[32]   Madubuonu N, Aisida SO, Ali A, Ahmad I, Zhao TK, Botha S, Maaza M, Ezema FI. Biosynthesis of iron oxide nanoparticles via a composite of Psidiumguavaja-Moringaoleifera and their antibacterial and photocatalytic study. Journal of Photochemistry and Photobiology B: Biology 2019; 199: 111601.
https://doi.org/10.1016/j.jphotobiol.2019.111601